LIQUEFACTION AND REMEDIATION OF SILTY SOILS

S. Thevanayagam[1], R. Nashed[1], T. Shenthan[1], and G. R. Martin[2]
[1]Univ. at Buffalo, SUNY, Buffalo, NY and [2]Univ. of Southern California, Los Angeles, CA.

ABSTARCT
Liquefaction of saturated loose granular sand and non-plastic silty sand deposits during seismic loading is one of the most dramatic threats to the safety of structures during earthquakes. Liquefaction-induced damages to highways and structures have been observed in almost all major earthquakes. Rational liquefaction screening tools and design methods for liquefaction remediation techniques are urgently needed to identify liquefaction prone areas and mitigate liquefaction-induced losses. Among many techniques, sand deposits densified by dynamic compaction (DC) and vibro-stone column (SC) are more resistant to liquefaction, and have performed well during earthquakes. Silty sand deposits appear to perform well when improved by either technique supplemented with wick drains. This paper presents a rational procedure to determine the level of densification achievable using each technique, with or without supplemental wick drains, for liquefaction mitigation of loose sand and non-plastic silty soils. It also presents a liquefaction screening method for these soils.

INTRODUCTION
A number of different silt-content dependent liquefaction screening methods (NCEER 1997) and densification techniques have been developed to mitigate liquefaction in loose saturated granular soils. Dynamic compaction (DC) and vibro-stone column (SC) are among the most field proven and commonly used techniques (Fig. 1). The DC technique involves high-energy impacts to the ground surface by systematically dropping heavy weights of 5 to 35 Mg from heights ranging from 10 to 40 m to compact the underlying ground using heavy crawler cranes (Lukas 1995). Vibro-stone column installation (FHWA 2001) process involves insertion of a vibratory probe with rotating eccentric mass and power rating in the vicinity of 120kW. The probe plunges into the ground due to its self-weight and vibratory energy, which facilitates penetration of the probe. Once the specified depth (depth of stone column) is reached, the probe is withdrawn in steps (lifts) of about 1m. During withdrawal of the probe, the hole is backfilled with gravel. During each lift the probe is then reinserted expanding the stone column diameter. This process is repeated several times until a limiting condition is achieved. Sand deposits densified by DC and SC are more resistant to liquefaction, and have performed well during earthquakes. Silty sand deposits appear to perform well when improved by either technique supplemented with wick drains (Dise et al. 1994, Andrews 1998, Han 1998, Luehring et al. 2001).

For both sands and silty sand sites, at present, there are no detailed analytical procedures available to analyze the effects of field DC and SC operational parameters and soil conditions to determine the densification and the degree of improvement achievable in the field. Current

practice for liquefaction screening, mitigation design, suitability assessment, and determination of optimum field operation parameters for DC and SC techniques rely mainly on field pilot tests, past experience based on case histories (Lukas 1995, Baez 1995). Attempts have also been made to use energy imparted DC and SC as a basis for ground improvement design (Lukas 1995, Green and Mitchell 2004). In the case of silty soils case histories of successful ground improvement are scarce. Advanced analytical techniques and computational tools need to be developed to aid liquefaction screening and mitigation design analyses taking into consideration site-specific soil conditions.

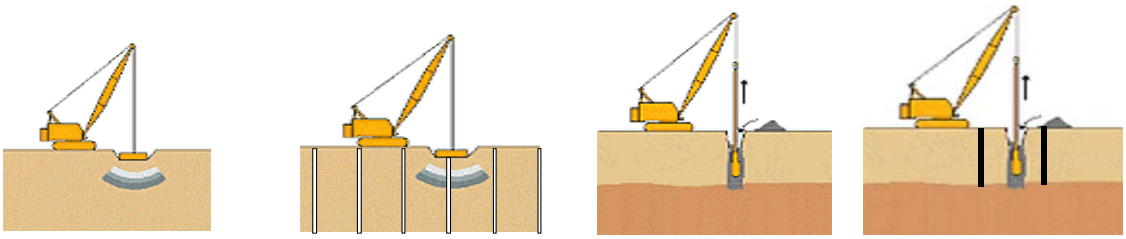

a) DC - sand sites b) DC - silty sand sites c) SC - sand sites d) SC - silty sand sites

Fig. 1 Dynamic compaction and Vibro-stone columns with and without wick drains

CONCEPTUAL FRAME WORK

It is recognized in the literature that liquefaction is a process involving energy dissipation due to frictional loss along grain contacts during cyclic loading leading to collapse of the soil structure and that this knowledge can be applied to develop methods for liquefaction screening and liquefaction mitigation design applications (Berrill, J.B. and Davis, R.O. 1985, Figueroa et al. 1994, Thevanayagam et al. 2000, Kayen and Mitchell 1997, Green and Mitchell 2004). The energy required to cause liquefaction depends on the density of packing of the grains. If the energy delivered to a deposit by an earthquake exceeds the energy required to cause liquefaction per unit volume of soil, the soil liquefies. It is also recognized that, in both improvement techniques, during the ground improvement works the ground vibrations induced by DC and vibratory probe as well as cavity expansion caused by repeated insertion of the vibratory probe cause rise in pore water pressures. If the energy delivered by DC or vibratory probe exceeds the energy required to cause liquefaction soil approaches liquefaction. Subsequent soil consolidation results in a highly denser arrangement of particles and the soil resistance to liquefaction increases. Repeated applications of DC and SC may help increase the soil density sufficiently to resist liquefaction due to a given earthquake. (Figs. 2-4). The level of DC or SC treatment required improve the ground to resist liquefaction for a given earthquake, in terms of impact or vibratory energy, spacing between impacts or stone columns, number of repeated impacts per location and time cycle between impacts, depends on the initial density of the soil, compressibility, hydraulic conductivity (and silt content), and provisions available for drainage of excess pore pressures induced during ground improvement works. When sufficiently developed, this framework can lead to development of energy-based liquefaction screening guidelines, and design methods for ground improvement to resist liquefaction.

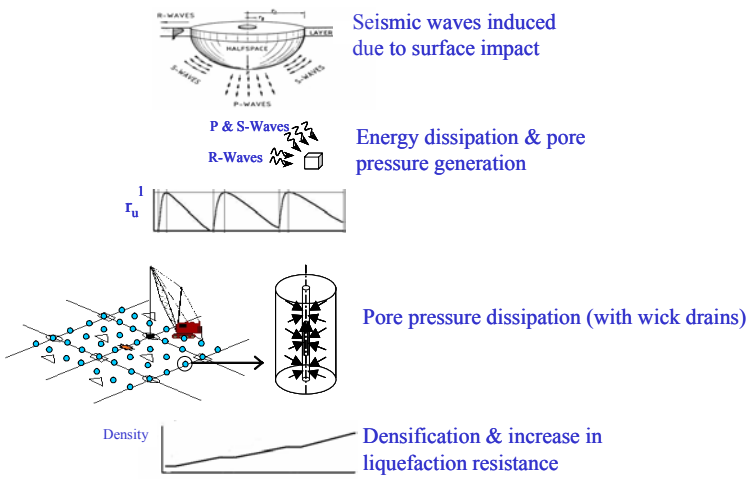

Fig. 2 Dynamic Compaction

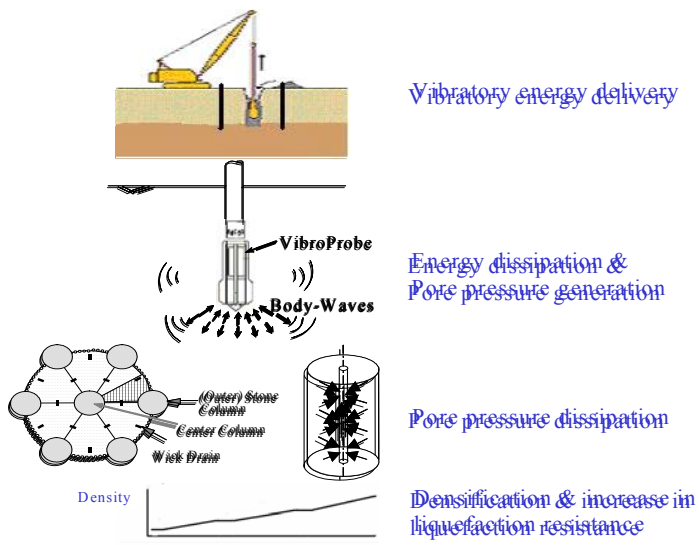

Fig. 3 Vibrostone colums

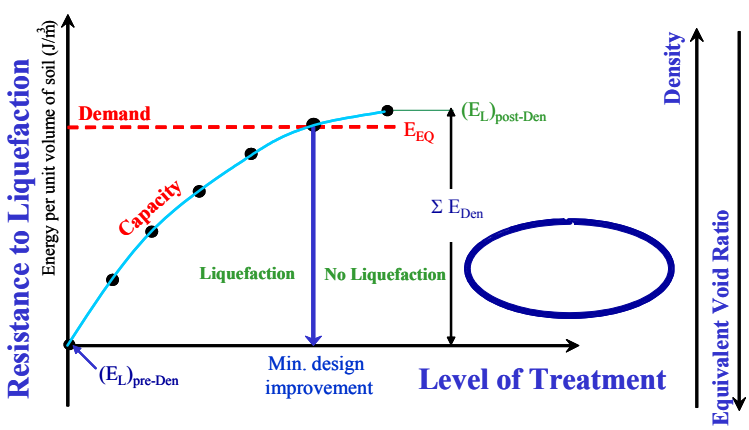

Fig. 4 Resistance to Liquefaction and Level of Treatment

NUMERICAL SIMULATIONS

Based on the above conceptual framework using energy principles governing soil liquefaction and soil densification by consolidation as the basis, a numerical simulation model has been developed to simulate the performance of soil deposits and determine density changes due to DC and SC (Shenthan et al. 2004). Simple attenuation relationships were used to estimate the time-histories of spatial distribution of energy dissipated in the soil during DC and SC. Experimental data based on energy principles was used to estimate the time-histories of spatial distribution of field pore pressures generated by DC and SC based on energy dissipated in the soil. Coupled consolidation equations were used to simulate soil consolidation to determine post-improvement soil density profiles. The influence of non-plastic fines content was taken into account in this simulation model by considering their effects on liquefaction resistance as well as on compressibility and hydraulic conductivity. Through collaborations with Advanced Geosolutions, Inc. and Hayward Baker, Inc. the model was successfully used to study and compare the observed field performance data with model predictions of post-improvement soil densities or penetration resistances at a number of field sites containing sands and non-plastic silty soils improved by DC or SC. Details of these comparisons are presented elsewhere (Shenthan 2005, Nashed 2005).

This framework has also been extended to develop a liquefaction screening method based on energy required to cause liquefaction, earthquake energy dissipated at a site, and cone penetration resistances (Thevanayagam and Ecemis 2006, Ecemis 2006).

Based on the success of this simulation model additional studies were conducted to develop simplified design charts to obtain the relationships between pre- and post-improvement soil densities improved by DC or SC supplemented with or without wick drains. A summary of the findings from this work are presented below. Stepwise design procedures and design examples using these design charts are presented elsewhere (Shenthan 2005, Nashed 2005).

Vibrostone Columns

In the case of vibrostone columns, numerical simulations were conducted to obtain the relationship between pre- and post-improvement densities for various uniform soil sites containing clean sands to non-plastic silty soils supplemented with or without wick drains. The diameter of stone columns was set at 0.9 m installed in a triangular pattern. Three different area replacement ratios were considered (A_r = 5.6, 10, and 22.5%). For all simulations, the power rating of the vibratory probe was set at 120 kW. In cases where supplementary wick drains were considered, the size of wick drains was assumed to be 100 mm x 5 mm with an equivalent diameter of 5 cm pre-installed at midpoints between stone columns. For convenient field applications, the results were converted in a form to present them in terms of equivalent normalized clean sand SPT blow counts $(N_1)_{60cs}$. The results were further grouped into three categories with soils at a pre-improvement equivalent normalized clean sand SPT blow count $(N_1)_{60cs}$ of 7, 11, and 16, respectively, each at three different area displacement ratios. Fig.5 shows these results, expressed in terms of post-improvement $(N_1)_{60cs}$ for soils with different hydraulic conductivities k, for a set of pre-improvement values of $(N_1)_{60cs}$ and A_r. The three figures in the first row (Fig.5a) represent soils with pre-improvement $(N_1)_{60cs}$ of 7, 11 and 16, respectively, improved using A_r =5.6%. The second and third rows (Figs.5b-c) are for soils improved using A_r =10% and 22.5%, respectively. Each figure has two curves, one for

improvement with stone columns only, and the other for improvement by stone columns supplemented with pre-installed wick drains.

Results indicate the following. Effectiveness of SC diminishes with a decrease in k (or with an increase in silt content). Area replacement ratio A_r has little influence on post-improvement densities for soils with hydraulic conductivities higher than 10^{-5}m/s. An increase in A_r up to about 22.5% extends the hydraulic conductivity of soils that can be improved by SC by nearly an order of magnitude to near 10^{-6}m/s. Pre-installation of supplementary wick drains has no influence on soil improvement for largely spaced stone columns with low A_r values. For closely spaced stone columns, with high A_r values exceeding about 20%, supplementary wick drains do influence soil improvement and extend the range of soils that can be improved by SC to include soils with high silt content and k values as low as in the range of 10^{-7}m/s to 10^{-8}m/s. The degree of improvement that can be achieved diminishes with a decrease in hydraulic conductivity, k.

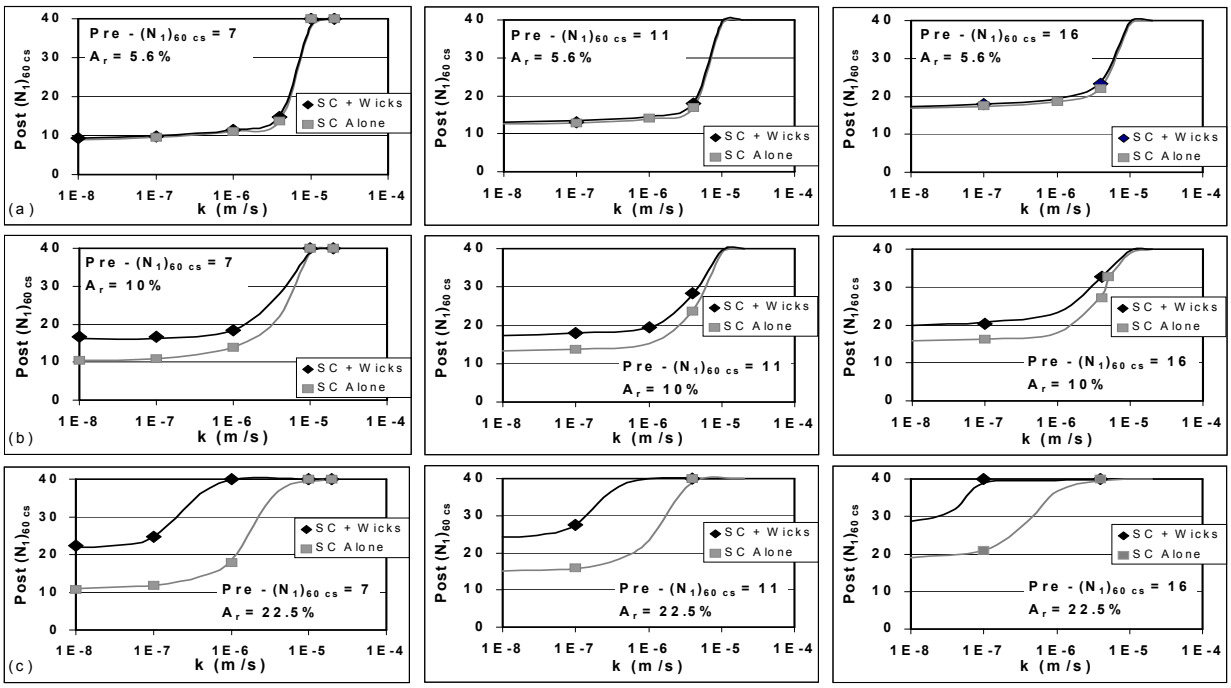

(SC + Wicks = vibro-stone column with wicks; SC = vibro-stone column without wicks)

Fig. 5. Vibro-stone columns – Post-Improvement design charts

Dynamic Compaction

In the case of dynamic compaction, numerical simulations were conducted to obtain the relationship between pre- and post-improvement densities for various uniform soil sites containing clean sands to non-plastic silty soils supplemented with or without wick drains. For all simulations, the impact grid pattern was assumed to be as shown in Fig.6. It involved three phases of impact, primary, secondary, and tertiary, respectively at the grid locations shown in this figure. The energy per impact (WH), impact grid spacing S, total number of impacts per grid point during each phase (N_I), wick drain spacing S_w, wick drain size, and time cycle between impacts T were varied for each simulation. Groundwater level was assumed to be at 2.0 m depth from impact surface.

Two sets of results are presented in Figs. 7 and 8. For these examples, the size of wick drains was assumed to be 100 mm x 5 mm with an equivalent diameter of 5 cm pre-installed at 1.5m spacing in a rectangular pattern. The number of impacts per grid location and the time cycle between impacts were set at $N_I = 12$ and $T = 2$ min., respectively. Fig. 7 shows the pre- and post-improvement $(N_1)_{60cs}$ profiles for two uniform soil deposits with pre-improvement $(N_1)_{60cs}$=7.5 and 16, respectively and impact grid spacing of S=15 m. The first two figures (Figs.7a-b) are for $k = 10^{-7}$ m/s, and the last two figures (Figs. 7c-d) are for and $k = 10^{-8}$ m/s. Each curve in these figures refer to the pre-improvement profile and post improvement profile for a different energy per impact *WH* of 100, 250, 500, and 750 Mg.m, respectively. Fig. 8 is for impact grid spacing of $S = 12$ m and energy per impact *WH* of 100, 250, and 500 Mg.m, respectively. Additionaldesign charts are presented in Nashed (2005).

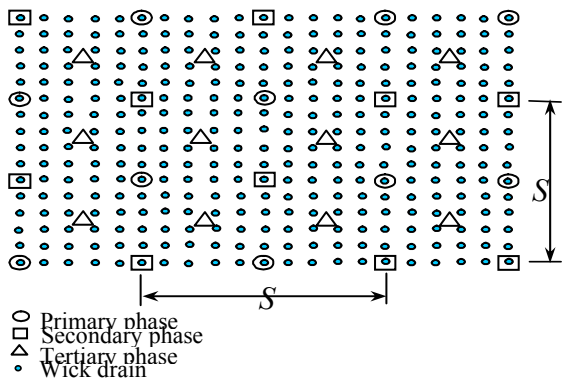

Fig. 6. DC Impact grid pattern

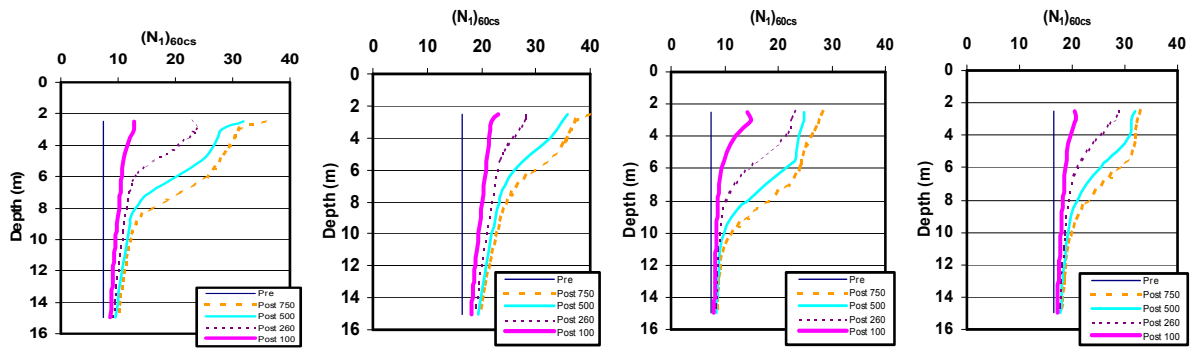

(a) k=10^{-7}m/s, *pre-*$(N_1)_{60cs}$ = 7.5 (b) k=10^{-7}m/s, *pre-*$(N_1)_{60cs}$ = 16 (c) k=10^{-8}m/s, *pre-*$(N_1)_{60cs}$ = 7.5 (d) k=10^{-8}m/s, *pre-*$(N_1)_{60cs}$ = 16

Fig. 7. Pre- and Post-improvement $(N_1)_{60cs}$ for $S = 15$ m (Post 750 = *WH* = 750 Mg. m)

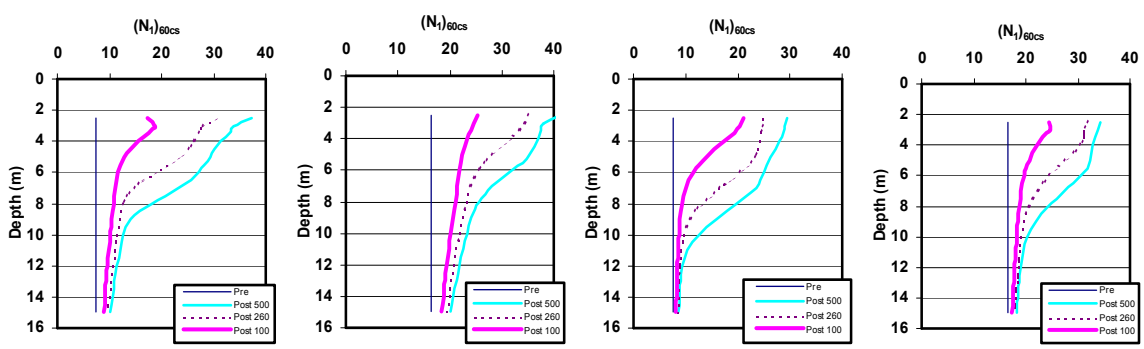

(a) k=10^{-7}m/s, *pre-*$(N_1)_{60cs}$ = 7.5 (b) k=10^{-7}m/s, *pre-*$(N_1)_{60cs}$ = 16 (c) k=10^{-8}m/s, *pre-*$(N_1)_{60cs}$ = 7.5 (d) k=10^{-8}m/s, *pre-*$(N_1)_{60cs}$ = 16

Fig. 8. Pre- and Post-improvement $(N_1)_{60cs}$ for $S = 12$ m (Post 500 =*WH* = 500 Mg. m)

Liquefaction Screening

In the case of liquefaction screening, simulation studies were conducted to determine the relationship between normalized energy required to cause liquefaction (E_L/σ'_c) and normalized cone penetration resistance (CPT) q_{c1N} with due consideration for the effects of silt content, hydraulic conductivity, compressibility on penetration resistance and liquefaction resistance in a uniform soil deposit (Thevanayagam and Martin 2002) (Fig.9a). Relationships were also developed for cyclic resistance ratio (CRR) applicable for an earthquake magnitude of 7.5 and CPT resistance and compared with silt-content dependent relationships (NCEER 1997) (Fig.9b). The simulation results are presented in terms of a ratio T (=cone diameter d x penetration speed v / coefficient of consolidation c_v). C_v decreases with increase in silt content (Thevanayagam and Martin 2002) and the ratio T increases. As silt content increases, the curves in Fig.9 shift to the left consistent with current field observations-based silt-content-dependent liquefaction screening methods (NCEER 1997). Detailed simulation procedures and analyses of these results are presented elsewhere (Thevanayagam and Ecemis 2006, Ecemis 2005).

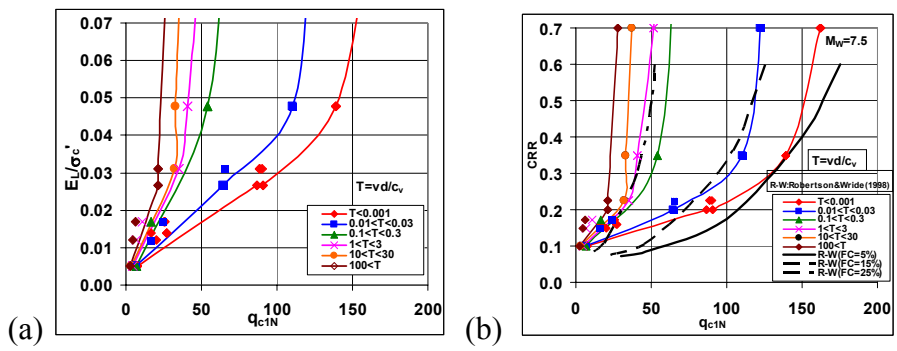

Fig. 9. Liquefaction Screening Charts for Sands and Silty Soils

CONCLUSIONS

Simplified design charts for determination of post-improvement penetration resistances of sands and non-plastic silty soils improved by dynamic compaction and vibro-stone columns have been presented. These design charts were developed based on energy principles governing liquefaction resistance of soils and soil consolidation due to repeated vibrations by dynamic compaction or vibro-stone columns. Results indicate that degree of improvement achievable by DC and SC at a site depends on hydraulic conductivity (or silt content), and on impact grid spacing, energy per impact, time cycle beween impacts in the case of DC, and on stone column spacing and wick drains in the case of SC. A significant increase in post-improvement $(N_1)_{60cs}$ can be achieved by SC and DC supplemented with pre-installed wick drains for soils with high silt content and low hydraulic conductivity as low as 10^{-7} to 10^{-8} m/s. In the case of SC, this effectiveness is reached only at small stone column spacing and high area replacement ratios exceeding about 20%. In the case of DC, the depth of influence for these soils can be as high as about 8 to 10 m and it is affected by energy per impact (*WH*), hydraulic conductivity, and pre-improvement $(N_1)_{60cs}$. The depth of influence decreases with a decrease in hydraulic conductivity and pre-improvement $(N_1)_{60cs}$. The charts presented herein are expected to advance the use of vibro-stone columns combined with wick drains to mitigate liquefaction potential in non-plastic silty soils, and reduce the reliance on expensive field trials as a design tool. Detailed design charts and design guidelines are reported in Shenthan (2005) and Nashed (2005). A soil-coefficient-of-consolidation-dependent liquefaction screening chart for sands and silty soils has

also been developed. Energy required to cause liquefaction has been correlated with cone penetration resistance. Cyclic resistance ratio (CRR) has also been correlated with cone penetration resistance. These charts need to be evaluated against case histories of liquefaction.

Acknowledgements
Financial support for this research was provided by MCEER Highway Project 094, sponsored by FHWA. J. Baez, Advanced Geosolutions, Inc., and Hayward Baker, Inc. provided field data.

References

Baez, J.I. (1995). "A design model for the reduction of soil liquefaction by vibro-stone columns" Ph.D. Dissertation, USC, Los Angeles, CA. 207 p.

Berrill, J.B. and Davis, R.O. (1985). "Energy dissipation and seismic liquefaction in sands: Revised model." *Soils and Found*., Tokyo, 25(2), 106-118.

Dise, K., Stevens, M.G., and Von Thun, J.L. (1994). "Dynamic compaction to remediate liquefiable embankment foundation soils", ASCE*, Geotech. sp. pub.*, No. 45, pp.1-25.

Ecemis, N. (2006). "Effects of fines on CPT resistance and liquefaction screening", *PhD Dissertation*, University at Buffalo, Buffalo, NY, *In preparation.*

Figueroa, J.L., Saada, A.S., Liang, L., and Dahisaria, M. N. (1994). "Evaluation of soil liquefaction by energy principles." ASCE, J. Geotech. Eng., 120(9),1554-1569.

FWHA (2001). "Stone columns" Ground Improvement Technical Summaries, II, Publication No. FHWA-SA-98-086R: (7-) 1-84.

Green, R. and Mitchell, J. K. (2004). "Energy-based evaluation and remediation of liquefiable soils", Geotrans 2004, Proc. Geotech. Eng. for transportation projects, ASCE, 1961-1970

Kayen, R.E. and Mitchell, J.K. (1997). "Assessment of liquefaction potential during earthquakes by arias intensity." *ASCE, J. Geotech. & Geoenv. Eng.,* 123(12), 1162-1174.

Luehring, R., N. Snorteland, L. Mejia, and Stevens, M. (2001). "Liquefaction mitigation of a silty dam foundation using vibro-stone columns and drainage wicks: a case history at salmon lake dam", Proc. 21st USSD annual meeting and lecture, Denver, CO.

Lukas, R.G. (1995) "Dynamic compaction", Federal Highway Admin., Rep. FHWA-SA-95-037.

Nashed, R. (2005). "Liquefaction mitigation of silty soils using dynamic compaction", *Ph.D. Dissertation*, University at Buffalo, Buffalo, NY, *In Review*.

NCEER (1997) Proc.NCEER Workshop on Evaluation of Liquefaction Resistance of Soils, Technical Report NCEER-97-0022, pp.1-40.

Shenthan, T., Nashed, R., Thevanayagam, S., and Martin, G. R. (2004), "Liquefaction mitigation in silty soils using composite stone columns and dynamic compaction", J. Earthq. Eng. and Eng. Vibrations, Vol.3, No. 1.

Shenthan, T. (2005) "Liquefaction mitigation in silty soils using composite stone column", *Ph.D. Dissertation*, University at Buffalo, Buffalo, NY, *In Review*.

Thevanayagam, S., Liang, J., and Shenthan, T. (2000). "A contact index for liquefaction potential analysis of silty/gravely soils." EM2000, Proc. 14th ASCE EMD Spec. Conf.*,* Tassoulas, ed., Austin, Texas.

Thevanayagam, S., and Martin, G.R. (2002). "Liquefaction in silty soils – screening and remediation issues." J. Soil Dyn. and Earthq. Eng., October.

Thevanayagam, S. and Ecemis, N. (2006). "Effects of fines on liquefaction screening using CPT resistance", Submitted to Proc. 8th National Conf. on earthq. Eng., San Francisco, April 2006.